

FIG. 1. SEM images of ZnO hexagram whiskers (a) with enlarged two hexagrams (b), enlarged side rods (c) and enlarged center rod array (d).

side nanorods making up the bundles are about $5\ \mu\text{m}$ in length and $250\ \text{nm}$ in diameter, with a big base attached on the angles of the disk. There is a bundle of nanorods with about $1\ \mu\text{m}$ in length and $250\ \text{nm}$ in diameter standing vertically on each disk surface [Fig. 1(d)].

Figure 2 shows the XRD pattern of the hexagrams. As indexed in the spectrum, all diffraction peaks match the hexagonal structure of wurtzite ZnO. It is noted that no obvious diffraction signal from the indium compound was observed, although there was about 20 at. % In_2O_3 mixed into the source. The EDX spectrum of the sample, detected over a large area [Fig. 1(a)], is shown as the insert in Fig. 2, to analyze the element content in the hexagrams. Indium signal is hardly observed in the EDX spectrum, although the calculated content of In is about 1 at. %. The results of XRD and EDX indicates that only a small amount of indium is doped into the lattice sites of ZnO. This phenomenon is understood by comparing the thermal dynamic properties of In_2O_3 and ZnO. The bond enthalpies of Zn–O and In–O in gaseous diatomic species are $159 \pm 4\ \text{kJ/mol}$ and $320.1 \pm 41.8\ \text{kJ/mol}$, respectively, and the calculated lattice energies of ZnO and In_2O_3 are $4142\ \text{kJ/mol}$ and $13928\ \text{kJ/mol}$,¹⁹ respectively. These parameters imply that

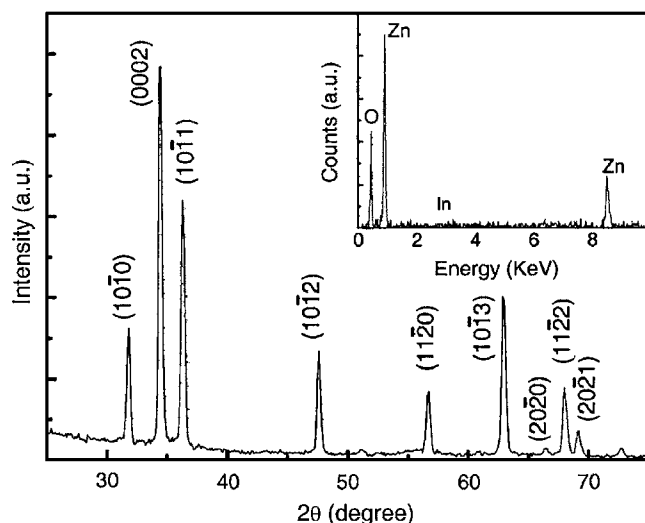


FIG. 2. XRD pattern of ZnO hexagram whisker, inserted by the EDX spectrum.

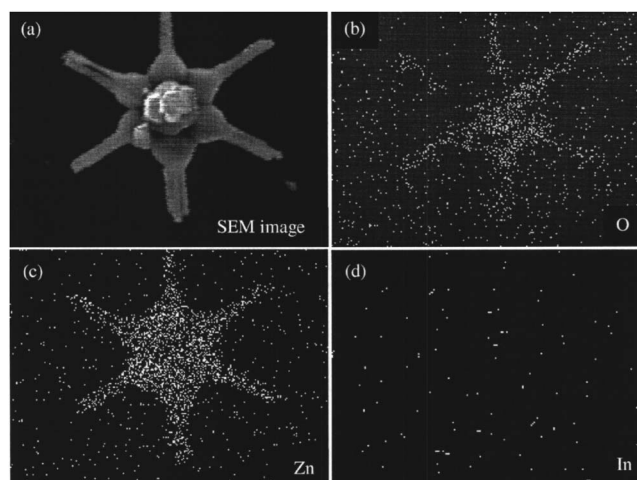


FIG. 3. SEM image (a) of an individual hexagram of ZnO and the corresponding element mappings of O (b), Zn (c) and In (d), respectively.

In_2O_3 is more difficult to be reduced into In vapor compared to ZnO being reduced into Zn, and the reduced Zn vapor is easier to bind with oxygen than In vapor.

The mixture of ZnO and In_2O_3 has been used to synthesize 3D hierarchical ZnO nanostructures by Lao *et al.*¹² In their experiment, the hexagonal In_2O_3 cores were formed first, and the secondary ZnO nanorods grew along the $[0001]$ direction from the side surface of In_2O_3 to form a heterostructure with sixfold symmetry in multiple rows. Similarly, Gao and Wang^{14,15} have also employed the mixture of ZnO and SnO_2 to synthesize 3D ZnO nanopropellers, which were found by first growing a hexagonal ZnO core along the $[0001]$ direction and enclosed by $\{2\bar{1}\bar{1}0\}$ surfaces, and later formed multilayer nanoblades along the sixfold symmetric equivalent directions of $\langle 2\bar{1}\bar{1}0 \rangle$ perpendicular to the core. In the present case, the hexagrams are homogeneously composed of ZnO and the core and side branches distribute almost on the same plane to form a quasi-2D structure due to the growth suppression in the $[0001]$ direction. Figure 3 shows the element mappings of an individual whisker measured by EDX. It can be seen that Zn and O are homogeneously distributed on the corresponding SEM image area of the hexagram. Only sparse dots appear randomly on the indium map, which is not enough to confirm the existence of indium. In order to understand the growth directions of the hexagram whiskers, SAED patterns were taken, respectively, from the edges of the core disk and the side rods by TEM, as shown in Fig. 4. The core disk presents clear hexagonal dif-

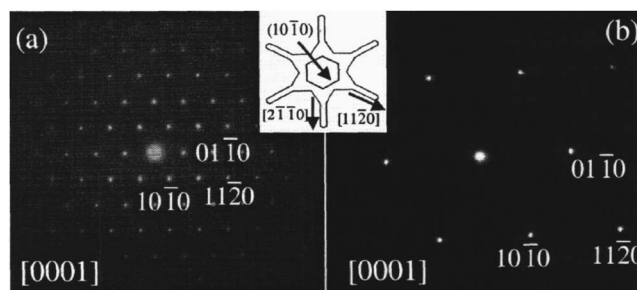


FIG. 4. SAED pattern taken from the edge of the core disk (a) and the side nanorod (b) of a ZnO hexagram from the $[0001]$ zone axis. The insert shows schematically the crystallographic planes and directions of the core disk and side nanorods.